

# Improving Grasp Planning Efficiency with Human Grasp Tendencies\*

Chang Cheng, Yadong Yan, Mingjun Guan, Jianan Zhang, and Yu Wang, *Member, IEEE*

**Abstract**—After a grasp has been planned, if the object orientation changes, the initial grasp may but not always have to be modified to accommodate the orientation change. For example, rotation of a cylinder by any amount around its centerline does not change its geometric shape relative to the grasper. Objects that can be approximated to solids of revolution or contain other geometric symmetries are prevalent in everyday life, and this information can be employed to improve the efficiency of existing grasp planning models. This paper experimentally investigates change in human-planned grasps under varied object orientations. With 13,440 recorded human grasps, our results indicate that during pick-and-place task of ordinary objects, stable grasps can be achieved with a small subset of grasp types, and the wrist-related parameters follow normal distribution. Furthermore, we show this knowledge can allow faster convergence of grasp planning algorithm.

**Index Terms**—Grasping, Multifingered Hands, Learning from Experience

## I. INTRODUCTION

Grasping is one of the most fundamental yet sophisticated tasks of the human hands. For simply picking up an object, a grasp requires object shape recognition, initial grasp planning, and sensory-motor control feedback from the human [1]. Despite many extant robotic hands can nearly restore the Degree of Freedom (DOF) of human hands, the lack of adequate grasp policies and sensory feedback hampers the attempt to plan and produce stable grasps.

Current grasp syntheses are classified into analytical and empirical ones [2]. The analytical approaches, such as [3] [4] [5], examine a mainly mathematical and computational problem [2]. Empirical grasp synthesis, such as [6], [7], [8], [9], are experience-based, and typically combines human grasp data with robotic learning policies to transfer observed grasps [10]. For both approaches, the complexity of anthropomorphic hands complicates grasp planning. Recent works have frequently modeled a human hand with over 20 DOF [11] [12]; with 6 additional DOF to define hand position and orientation, the grasp configuration space contains nearly 30 dimensions when fully parameterized. This high dimensionality calls for simplification.

\*Research supported by “National Key R&D Program of China” under grant 2017YFA0701101.

Y. Yan, M. Guan, J. Zhang, and Y. Wang (corresponding author) are with the School of Biological Science and Medical Engineering, Beihang University, Beijing 100191, China (fax: 8610-82315554; email: adam7217@qq.com; mingjunguan7@163.com; baby0303zjn@buaa.edu.cn; wangyu@buaa.edu ).

C. Cheng is with the Department of Mathematics and Computer Science, Colorado College, CO 80946, USA (email: d\_cheng@coloradocollege.edu)

In the discrete sense, the seminal work by Napier [13] divided common grasps into “precision” and “power” grasps, which is expanded into 16 more specific types by Cutkosky [14], and later into 33 by Feix et al. [15]. These classifications simplify the process of transferring human grasps to robots for grasp synthesis. For example, Ekvall et al. constructed a grasp planning system where a grasp pre-shape is provided, and the robot searches for an approach vector to complete the grasp [16]. Using algebraic methods, Santello et al. [17] used data-gloves to measure joint angles during grasps and represented postural synergies in human hands as eigenvectors. This reduced the hand configuration space to 3 dimensions while preserving 70% of individual joint variation. These synergies have shown success in reducing the control complexity of both fully actuated [18] and underactuated [19] anthropomorphic hands. Building on the work of Santello et al., [20] and [21] have developed grasp planning algorithms in reduced postural spaces. While these two algorithms are based on different frameworks: simulated annealing and reinforcement learning, both algorithms demonstrated that stable grasps can be planned and optimized in significantly reduced grasp subspaces.

Aside from finger specific parameters, wrist-related parameters are also essential to a grasp and need simplification. Balasubramanian et al. showed that when human-planned grasps outperform computer-planned ones, the difference often lie in the wrist orientation [22]. When postural synergies are used to parameterize hand postures, a grasp is often described by 9 variables: 3 for eigenvalues and 6 for wrist position and orientation. Thus, searching efficiently in the wrist transformation space may be important to building fast grasp planning algorithms. Heuristics have been developed for this purpose. In the system developed by Ciocarlie et al., a magnet tracker operated by human is used to provide a rough search area for the wrist transformation [23]. Li et al. first generated hand postures according to object features, then aligned the hand to the object surface [24]. Huebner et al. created bounding boxes for the objects and determined the hand orientation with faces and edges of the boxes [25]. Bohg et al. aligned the approach vector of the hand with the object surface normal and approximated the approach distance in a fixed range [26]. While these heuristics bound these algorithms in reasonable time, some parameters lack validation. Such as the orientation and magnitude of the search direction vector in [23], the approach distance in [26], and the widely used method of generating wrist transformations from object surface. These parameters make logical sense, but some empirical validation, possibly through statistical analysis of human grasps, may be meaningful.

This letter aims to provide a grasp-search optimization model from human grasps. The work in this paper is inspired

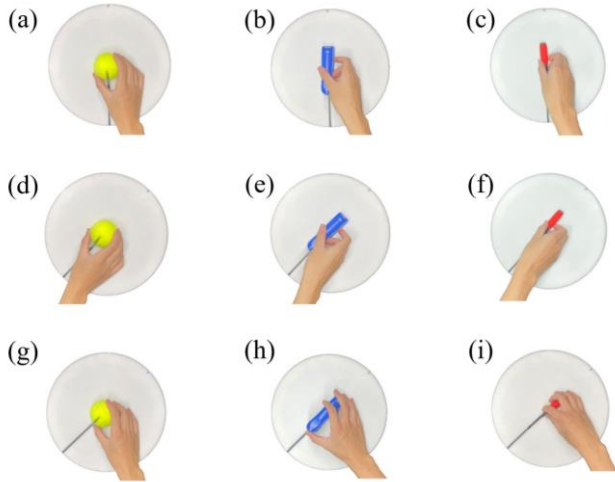


Fig. 1. Human grasps of objects under different orientations. A tennis ball (a), (d),(g), a stapler (b), (e), (h), and a screw driver (c), (f), (i) are grasped respectively. Grasps in (a-c) represent the grasps for the object in initial orientation, (d-f) represents the grasps where the hand rotates with the object, (g-i) are grasps that humans tend to choose for the new object orientation.

by the occurrence that due to object structural similarities and the adaptability of human hands, when object-orientation changes, commensurate change in the hand is not required to achieve stable grasps. For instance, in Fig. 1, the objects are rotated 45 degrees clockwise from (a-c) to (d-i). In Fig. 1(d-f), the hand rotates with the object to replicate the grasps in (a-c). Interestingly, due to the structural symmetries of the objects and adaptability of the human hand, non-identical but stable grasps can be produced with little transformation. The relative geometrical feature of a tennis ball to the grasper is identical under all object orientation, so when a tennis ball rotates, a stable grasp can be produced without adjusting the previous grasp at all, which is shown in between (a) and (g). For rather irregular objects, different levels of changes are required. Between (b) and (h), the wrist mostly remains static while the finger configuration changes to adapt to the new object orientation. From (c) to (i), the finger configuration remains fixed while the wrist rotates, but the direction and angle of wrist rotation does not match the rotation of the object. Grasps in Fig. 1. manifest the nonlinear nature of grasp planning; furthermore, it preliminarily supports the hypothesis that stable grasps may be achieved using a subspace of the wrist transformations.

In this paper, we experimentally explore change in human grasps for everyday objects with respect to change in object orientation. Such relationship is organized into the Grasps Under Varied Object Orientation Dataset (GUVOOD). Based on such dataset, a grasp planning efficiency improvement model is proposed and implemented in a state-of-the-art grasp planning algorithm. The original algorithm and proposed algorithm are then benchmarked on 8 ordinary objects.

## II. MATERIAL AND METHODS

This section describes the methods employed to investigate the relationship between human-planned stable grasps and object orientation. Human subjects are instructed to grasp everyday objects under different orientations, and the change of the grasps with respect to changes in object

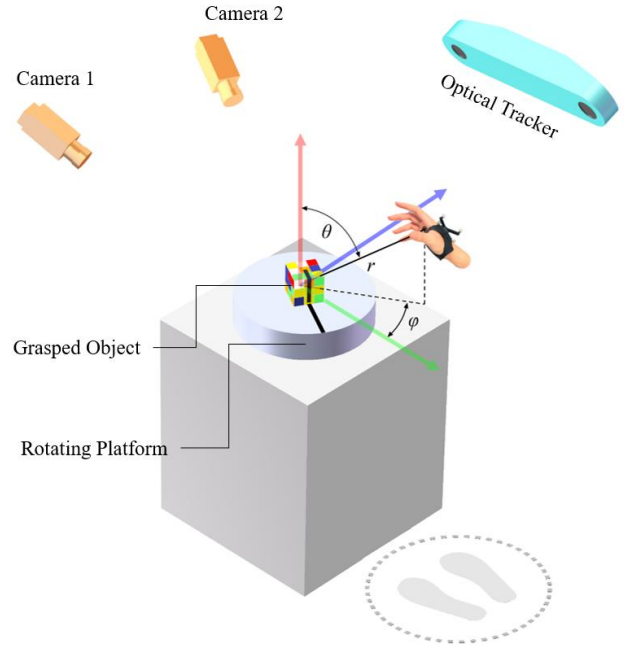


Fig. 2. Instruments in the experimental setup. The grasper stands opposite to the two cameras during the experiment.

orientation is measured. The experimental setup is shown in Fig. 2. An optical tracking system is employed to record the spatial transformation of the wrist, and two cameras are employed to register the hand posture. Therefore, any observed grasp is parameterized by seven variables:  $\varphi, \theta, r, R_x, R_y, R_z, t$ ; whereas  $\varphi, \theta$ , and  $r$  describe the wrist position in polar coordinates,  $R_x, R_y$ , and  $R_z$  describe the wrist rotation, and  $t$  is the manually labeled grasp type from the Cutkosky grasp classification [14]. For each subject, the objects are rotated to and grasped under 8 different orientations that are evenly spaced.

### A. Grasped Objects

The object selection aims to include daily objects with varying sizes and shape complexities. A total of 60 objects are chosen and are displayed in Fig. 3, among which 21 and 15 have counterparts from [17] and the YCB dataset. It is worth noting that some objects have alternative ways of being placed on a surface; Fig. 3. displays the unique way each object is presented to the graspers.

Certain objects with symmetrical properties would be isomorphic to itself under other orientations. Take a tennis ball, for example; all rotations of a tennis ball yield the same geometric properties relative to the grasper. To investigate the effect of geometric symmetry on human-produced grasps, we categorize the grasped objects into three groups: solids of revolution (SoRs), cuboids, and irregular objects. SoRs refer to objects whose 3-D model can be obtained through rotation of a plane curve around a centerline, i.e., spheres and cylinders. These objects are isomorphic under all rotations of themselves about the centerline orthogonal to the platform plane. The cuboids are objects that can be approximated to cubes or rectangular boxes. The irregular objects are neither SoRs nor cuboids.

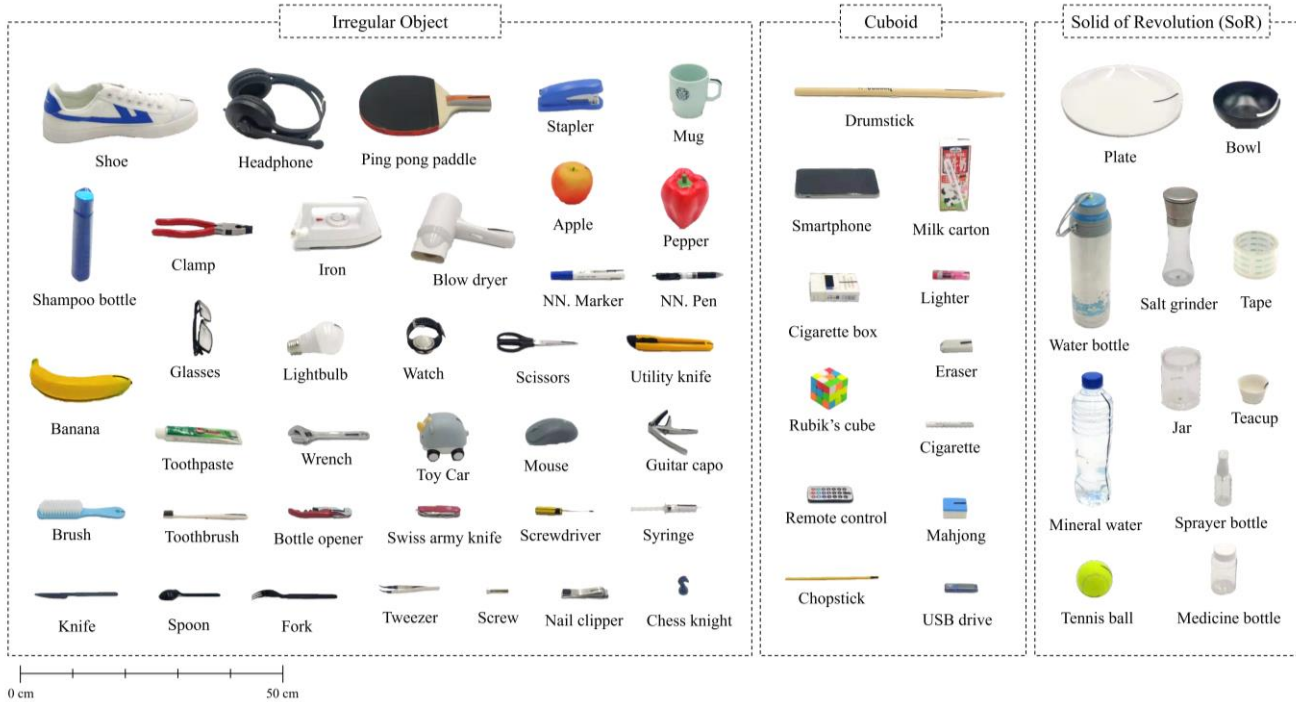


Fig 3. Images of actual objects used for the experiment. All objects are drawn to scale. The objects are classified into three categories by degree of symmetry: irregular objects, cublids, and solids of revolution (SoRs). For many of the objects above, there are multiple ways to place them on a surface. For example, a bowl can be placed with the opening facing up or down. In this experiment, the ways the objects are presented above are how they are placed during the experiment.

### B. Protocol

Previous work in the field has shown that grasps are strongly correlated with the usage of the objects [13]. This phenomenon may become a disturbance to this study. For instance, a syringe is commonly held with the index and middle finger on the barrel and the thumb at the end of the plunger for injection, but this is not the most stable and convenient way to grasp a syringe. To avoid potential bias occurring from object application, we instruct the subjects to neglect the conventional usage of an object and concentrate explicitly on the task of pick-and-place before experiments begin.

The subject sits roughly 0.4 meters away from the center of the rotating platform. The experiment begins as an operator puts the first object in the center of the platform. The subject is instructed to grasp the object and attempts a pick-up to demonstrate the success/failure of the grasp. The operator records the grasp along with the evaluation, and the subject

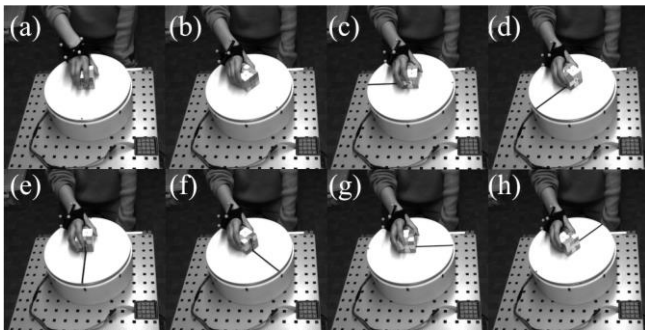


Fig 4. Example images of the recorded grasps under 8 different object orientations during the experiment.

places the object back on the platform. The operator rotates the platform by 45 degrees counterclockwise and repeats the steps above under the updated object orientation. Once grasps under all eight rotational orientations have been recorded, the next object is placed on the platform. This process repeats until grasps of all 60 objects have been recorded. Figure 4. shows sample data collected from one subject.

### III. THE GRASP DATASET

Throughout the experiments, twenty-one righthanded and seven lefthanded subjects participated, and 13440 grasps were added to the GUVOOD overall. Among all grasps, 203(1.51%) contain ambiguous wrist transformation, and 86(0.63%) grasps failed. The ambiguous grasps resulted from the loss of sight of the reflective tracker, and the failed grasps mainly occurred on flat and heavy objects such as wrench (48 fails) and knife (20 fails). This section presents and discusses the unambiguous, successful grasps in the GUVOOD.

#### A. Wrist Position

A scatter plot of the palm positions in the GUVOOD is shown in Fig. 5(a, b). For both left and right-handed graspers, the grasps congregate in a single cartesian octant. The center of the point clouds also exhibits a higher density of grasps. Fig. 5(e). displays the distribution of the  $\varphi$ ,  $\theta$ , and  $r$  used to parameterize grasp locations. The  $\theta$ , and  $r$  distributions of the left and right-handed graspers are near identical and the  $\varphi$  variables resemble the reciprocal of the other. The frequencies of all three position parameters bear resemblance to the standard normal probability density function (PDF) calculated from the mean and standard deviation (STD) of the variables except the  $r$  frequency is slightly left-skewed. A possible

cause of the skewness is that the reflective tracker is put on the back of the hand. Because  $r$  essentially measures the distance from the hand to an object, and all grasps are made where the palm faces the object, the  $r$  parameter becomes slightly biased by the thickness of the palm.

### B. Wrist Orientation

Because the left and right-hand mirror each other, two different coordinate systems are built for the left and right hand to allow more comparable data representation, shown in Fig. 5(c, d). Both coordinate systems have the x-axis pointing above the back of the hand. For the left hand, the z-axis points

towards the thumb and the y-axis points towards the wrist. For the right hand, the y-axis points to the thumb, and the z-axis to the wrist. The  $R_x$ ,  $R_y$ ,  $R_z$  rotations are then calculated in XZY order for the left hand and XYZ order for the right. Similar to the frequency of the positional parameters, the wrist orientation parameter frequencies for the left and right-hand mirror each other, and the distribution resembles standard normal PDF.

### C. Grasp Types

The grasps produced in the experiment are manually

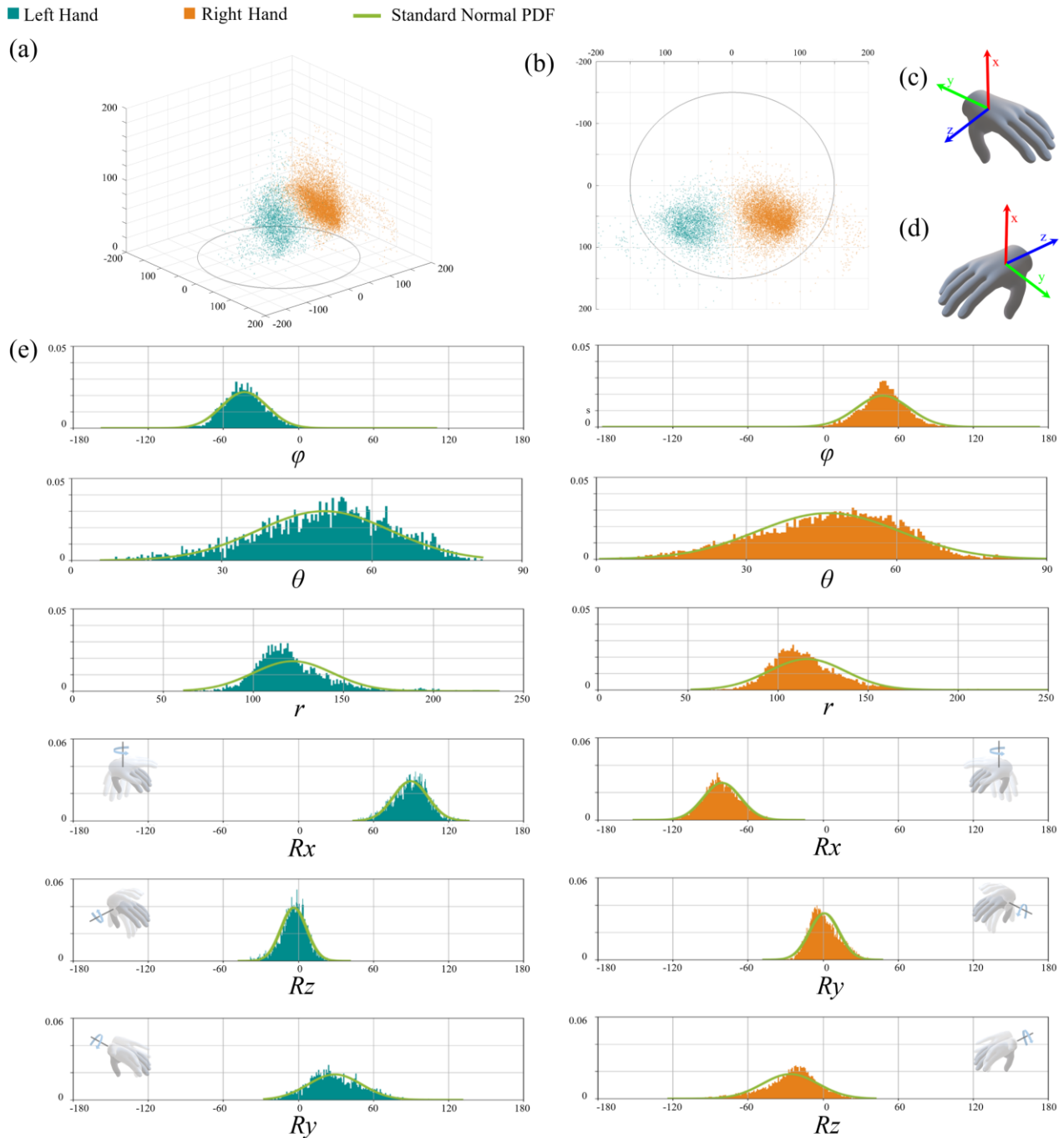


Fig 5. Distribution of the wrist transformation parameters from the grasp dataset, the graph legends are displayed above (a). (a) and (b) are scatterplots of the wrist positions, (c) and (d) display the coordinate system used for the left and right hand, respectively. (e) shows the frequency graphs for the corresponding parameters.

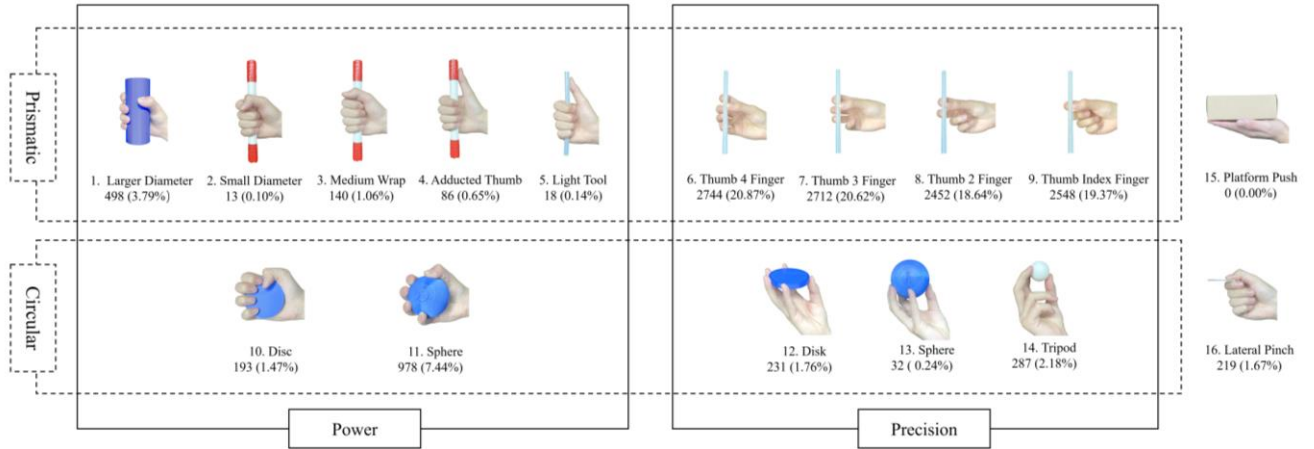


Fig. 6. Frequencies and of different grasps employed according to Cutkosky’s classification. The left number below each grasp indicate the number of occurrences, and the number in parentheses indicate the percentage calculated from the successful, unambiguous grasps.

classified by the taxonomy proposed in [14], and the results are shown in Fig. 6. The most frequent grasps observed are the four precision prismatic grasps, which together account for 79.5% of total grasps. Precision and power grasps each make up 85.4% and 14.6% of the dataset. Such dominance of precision over the power grasps is more drastic than a comparable study done by Cini et al., which collected 62.0%, 7.6%, and 30.4% for precision, intermediate, and power grasps respectively [27]. This difference may be due to object and task selection and the additional category of intermediate grasps from [27].

#### D. Object Geometry

Section II. A. divides the grasped objects into three categories: SoRs, cuboids, and irregular objects. It is hypothesized that the range of  $\varphi$  should be larger for irregular objects than cuboids than SoRs. Table I displays the standard deviation for the hand position variables. The  $\theta$  variable is consistent across object groups while the  $\varphi$  and  $r$  STDs agree less. The  $r$  variable parameterizes the distance from the wrist to the origin; thus its STD implies the variation of object size in a group. The SoRs contain some of the largest and smallest objects: plate, water bottle, teacup, sprayer bottle. In contrast, object size differences in cuboid and irregular object groups are less apparent, which justifies the diverse STD for  $r$ . Unlike  $r$ , the STD for  $\varphi$  grows from SoRs (12.12, 12.72) to cuboids (17.48, 15.74) to irregular objects (23.94, 20.02). The axis that the objects are rotated around, the object centerline orthogonal to the platform, is also the axis which the  $\varphi$

parameter rotates around. Thus, the STD of  $\varphi$  across different groups is associated with the degree of rotational symmetry among a group of objects. Since the magnitude of rotational symmetry decreases from SoRs to cuboids to irregular objects, the corresponding  $\varphi$  STD shall increase.

#### IV. GRASP OPTIMIZATION MODEL

In the context of this paper, the efficiency of a planner is defined as the ability to reach low energy in few iterations. Based on the experimental outcomes of the previous section, we construct an optimization model for improving grasp planning efficiency. To find stable grasps, planning algorithms typically generate and rank possible grasps then return grasps with high evaluations; this procedure is also termed the offline-generation paradigm [10]. This makes the grasp generation function’s ability to generate apt candidates essential to the efficiency of the planning algorithm. One way to optimize offline generation algorithms is to enable the grasp generation function to sample grasps that are more likely to become the final grasp, which should allow the algorithm to converge in fewer iterations. The simulated annealing grasp planner from [20] is a state-of-the-art grasp planner that 1) work well on hands with high DOF, 2) incorporates stochasticity to avoid escape minima, 3) has been shown to generate acceptable grasps stably. For these reasons, the simulated annealing planner is chosen as the benchmark. This section introduces one method the GUVOOD can be applied to this algorithm.

The structure of the simulated annealing method is similar to the offline-generation paradigm; a key difference is that it escapes local minima by using a probabilistic function to decide whether the algorithm should jump to a new grasp. For a thorough introduction of the method, we refer readers to [20]. While the simulated annealing method works well, its grasp generation might be “too random” and contains room for improvement. The GUVOOD indicates that most human grasp for ordinary objects are within a grasp subspace, and many parameters tend to follow a normal distribution. If we apply this human-derived information to the grasp generator, the generator should return grasps that are more likely to be planned by humans. Given that humans are currently

TABLE I. WRIST POSITION PARAMETER STANDARD DEVIATION

|       |           | SoRs  | Cuboid | Irregular Objects |
|-------|-----------|-------|--------|-------------------|
| Right | $\varphi$ | 12.12 | 17.48  | 23.94             |
|       | $\theta$  | 13.71 | 13.19  | 13.925            |
|       | $r$       | 27.10 | 13.82  | 18.75             |
| Left  | $\varphi$ | 12.72 | 15.74  | 20.02             |
|       | $\theta$  | 12.48 | 12.11  | 13.30             |
|       | $r$       | 27.20 | 14.42  | 19.88             |

TABLE II. CONFIDENCE INTERVALS OF THE WRIST TRANSFORMATION PARAMETERS

|            |           | mean   | 99% Interval |        | 95% Interval |        | 90% Interval |         |
|------------|-----------|--------|--------------|--------|--------------|--------|--------------|---------|
|            |           |        | Lower        | upper  | lower        | upper  | lower        | upper   |
| Right Hand | $\varphi$ | 48.06  | -22.27       | 113.07 | 8.86         | 85.17  | 16.95        | 77.55   |
|            | $\theta$  | 46.45  | 9.09         | 80.63  | 16.45        | 70.75  | 21.37        | 67.36   |
|            | $r$       | 116.30 | 75.51        | 209.60 | 84.56        | 168.68 | 89.38        | 154.43  |
|            | $R_x$     | -80.63 | -118.61      | -39.73 | -108.32      | -50.10 | 103.71       | -55.52  |
|            | $R_y$     | 1.15   | -24.17       | 33.47  | -18.52       | 26.66  | -15.85       | 22.86   |
|            | $R_z$     | -25.97 | -94.19       | 21.46  | -78.81       | 12.00  | -68.89       | 6.62    |
| Left Hand  | $\varphi$ | -42.92 | -95.75       | 14.76  | -75.97       | -7.36  | -68.67       | -14.17  |
|            | $\theta$  | 50.49  | 13.17        | 77.02  | 21.32        | 73.19  | 26.16        | 70.87   |
|            | $r$       | 122.05 | 79.33        | 212.86 | 89.63        | 184.16 | 95.01        | 162.166 |
|            | $R_x$     | 89.89  | 52.02        | 126.42 | 61.49        | 115.64 | 66.23        | 110.94  |
|            | $R_y$     | 29.40  | -19.11       | 85.85  | -9.48        | 73.26  | -4.64        | 66.24   |
|            | $R_z$     | -3.48  | -35.80       | 21.01  | -26.56       | 15.14  | -21.34       | 11.89   |

substantially better at planning grasps than machines, this approach may improve the planned results.

To incorporate the wrist positional and rotational parameters, the 90% interval of  $\varphi$ ,  $\theta$ ,  $r$ ,  $R_x$ ,  $R_y$ ,  $R_z$  from Table II are set as upper and lower bounds for the corresponding variables. However, for the finger configuration parameters, because the GUVOOD registers grasp finger configurations in discrete forms, it cannot be directly applied to the algorithm that adjusts finger configuration in continuous space. To accommodate this difference, we extracted the most frequent grasp types from the GUVOOD, and the eigengrasps are adjusted to allow straightforward execution of these grasp pre-shapes. Eight grasps are extracted, whose indexes are: 6, 7, 9, 8, 11, 1, 14, and 12. These grasps imply independent flexion for all fingers, along with some abduction is needed. Therefore, the eigengrasps are set as the following,

EG1: abduction of index, middle, ring, little finger,

EG2-5: flexion of index, middle, ring, little finger respectively,

EG6-7: rotation and flexion of the thumb, respectively.

## V. EXPERIMENTAL EVALUATIONS

This section compares the proposed modified simulated annealing algorithm with the benchmark algorithm. GraspIt! is an open-source grasp planning environment that enables energy calculation and visualization. Both algorithms are implemented and tested under GraspIt! on the same laptop computer with a 2.2Ghz Intel CPU. A human hand with 20-DOF is employed as the grasping effector. Because the tasks of grasp planning vary on different objects and the simulated annealing method is non-deterministic, the algorithms are performed ten times on eight different items with different levels of geometric complexity to ensure fairness. Among the grasped objects, four are primitive shapes: a cube, a sphere, a tube, and an octahedron; the other four include a banana, a lightbulb, a stopwatch, and a blow dryer. The grasp scene contains a table with the object located

at the origin, and the hand is initially placed slightly above the object. Both algorithms perform 40,000 iterations, as this has been indicated as the point the algorithm converges, and the lowest energies at different stages are recorded. The preset-contact measure is chosen as the energy calculation function, which predefines frequent contact points on the human hand during grasping and measures the distance from contact points to the object surface normal. This function is chosen because it can generate acceptable grasp quality measure in a short amount of time, which makes it a practical heuristic for real-world applications. The change in energy at different stages of the algorithms are plotted in Fig. 7, the average time for completion is plotted in Fig. 8, and Fig. 9. displays examples of the planned results. The legend for Fig. 7. and Fig. 8. is displayed above Fig. 7.

It can be observed that the proposed algorithm is able to reach lower energies after 40,000 iterations consistently. For all objects, the proposed algorithm reduces the energy substantially during the initial stage (iterations 0-10000) while the benchmark planner does not except for on the blow dryer. A property of the simulated annealing process is that it initially searches in a relatively large space, then progresses to fine-tuning in later iterations. The “sharp drop” that is more prevalent in the proposed planner may be accounted for by its bounded search space. The grasp variable bounds provided by the GUVOOD keeps the grasp generation in regions with a high density of human-preferred grasps. Thus, it has a higher probability of reaching low energy in early iterations. As the algorithm continues, the search space shrinks, and the benefits of the bounds lessen. After the iteration where the search space becomes within the bounds, the effect of the bounds disappears, and the two algorithms become essentially the same, which may account for the similarity between the two converging patterns from mid to late-stage (10000-40000).

On average, the benchmark and proposed algorithm took 34.63 and 33.84 seconds to complete 40,000 iterations on the eight objects tested. The proposed algorithm reached the final energy of the benchmark after 6,000 iterations at best on the

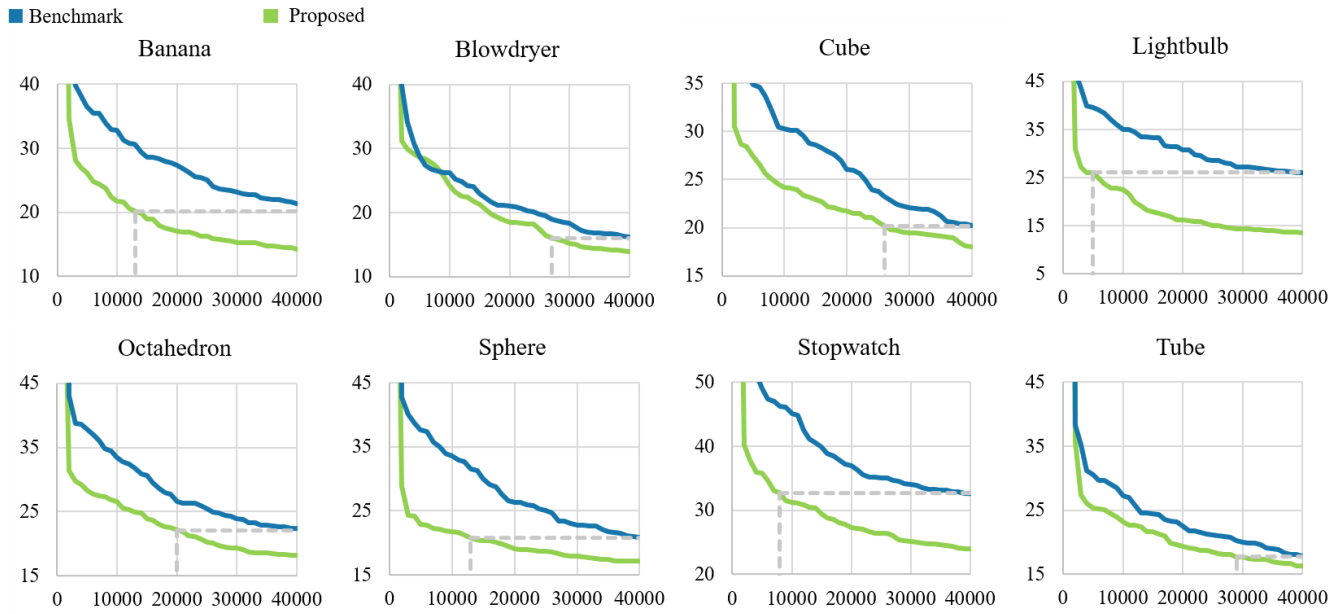


Fig 7. The convergence progression of the planners. The energy of the planners for different objects are averaged at different iterations. The horizontal axes represent iterations, and the vertical axes indicate the energy.

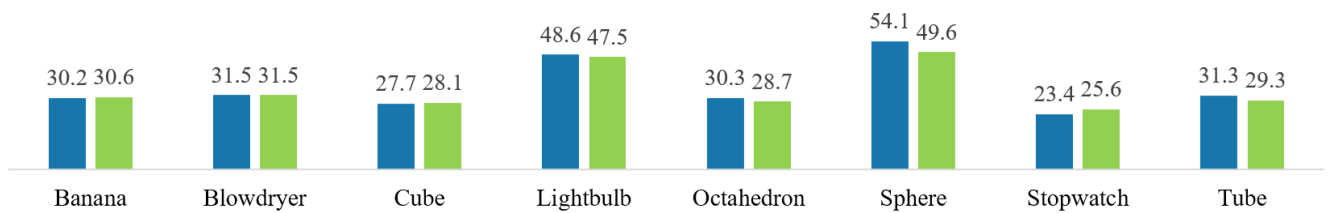


Fig 8. The average elapsed time of the two grasp planners.

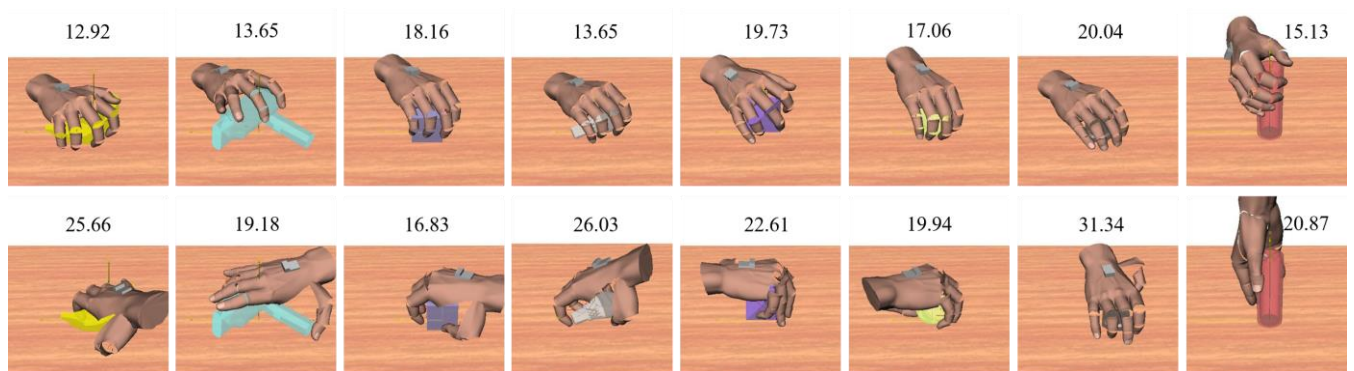


Fig 9. Examples of the planned grasps from both algorithms after 40,000 iterations, the energy of each grasp is displayed above the corresponding grasp. Grasps in the first row are planned by the proposed planner, and the second row contains grasps planned by the benchmark planner. The wrist transformation of grasps planned by the proposed planner seem more homogenous than the ones planned by the benchmark, this is due to the bounds applied.

lightbulb and 29,000 iterations at worst on the tube. It reaches the energy of the benchmark after 17750 iterations on average. The proposed algorithm can appreciably converge to lower energies for this set of test objects without increasing the computation time per iteration.

## VI. DISCUSSION AND CONCLUSION

This letter investigated a hypothesis inspired by an observation of human grasp patterns. After such hypothesis has been backed by experimental results, it is utilized to improve grasp planning efficiency. With a collection of 13,440 grasps, we discover that the transformation parameters

of the grasps across different graspers, objects, and orientations tend to follow the normal distribution. Usually, sampling of a population that occurs “naturally” would yield a normal distribution. Examining the “naturalness” of grasp parameters is beyond the scope of this paper but is worth researching in the future. The study in this paper takes a similar approach as past attempts to reduce grasp complexity: deriving grasps from humans. Contrary to using Principal Component Analysis or Machine Learning methods, the grasp simplification policies derived from this study are simple to explain: the bounds for  $\varphi$ ,  $\theta$ ,  $r$ ,  $R_x$ ,  $R_y$ ,  $R_z$  are such because 90% of the human-planned grasps are within this range, the eigengrasps are such because it is necessary to perform the

most frequent grasp pre-shapes. The disadvantage of this approach is that the learning capabilities of humans are limited, and machines may be able to identify patterns that seem inconspicuous to humans. Therefore, reexamining the GUVOOD with machine learning, deep learning, or algebraic technique may be future work that stems from this letter.

When the grasp pre-shape information from the GUVOOD is applied to the planner, the discrete labels are converted to the continuous representation of eigengrasps. Such transformation was done because the benchmark planner searches in a continuous space. However, when applying the GUVOOD in other scenarios, sampling finger configurations in a discrete set of grasps is a possible alternative, as [28] has created a probabilistic grasp planner based strictly on grasp types. This paper only introduces one approach to take advantage of the GUVOOD; creating a probabilistic grasp planner is among many other alternative future implementations of this dataset.

#### ACKNOWLEDGMENT

The authors would like to express their gratitude to the developers who created GraspIt! that provided the platform for implementing and testing grasp algorithms in this study.

The experimental protocol was established, according to the ethical guidelines of the Helsinki Declaration and was approved by the Human Ethics Committee of Beihang University.

#### REFERENCES

- [1] R. S. Johansson and K. J. Cole, "Sensory-motor coordination during grasping and manipulative actions," *Curr. Opin. Neurobiol.*, vol. 2, no. 6, pp. 815–823, Dec. 1992, doi: 10.1016/0959-4388(92)90139-C.
- [2] A. Sahbani, S. El-Khoury, and P. Bidaud, "An Overview of 3D Object Grasp Synthesis Algorithms," *Robot. Auton. Syst.*, vol. 60, pp. 326–336, Mar. 2012, doi: 10.1016/j.robot.2011.07.016.
- [3] J. Ponce, S. Sullivan, A. Sudsang, J.-D. Boissonnat, and J.-P. Merlet, "On Computing Four-Finger Equilibrium and Force-Closure Grasps of Polyhedral Objects," *Int. J. Robot. Res.*, vol. 16, Dec. 1995, doi: 10.1177/027836499701600102.
- [4] S. El-Khoury and A. Sahbani, "On computing robust N-finger force-closure grasps of 3D objects," 2009, p. 2486. doi: 10.1109/ROBOT.2009.5152272.
- [5] J. Li, H. Liu, and H.-G. Cai, "On computing three-finger force-closure grasps of 2-D and 3-D objects," *IEEE Trans. Robot. Autom.*, pp. 155–161, Mar. 2003, doi: 10.1109/TRA.2002.806774.
- [6] M. A. Roa, M. Argus, D. Leidner, C. Borst, and G. Hirzinger, "Power grasp planning for anthropomorphic robot hands," *Proc. - IEEE Int. Conf. Robot. Autom.*, pp. 563–569, May 2012, doi: 10.1109/ICRA.2012.6225068.
- [7] J. Tegin, S. Ekvall, D. Kragic, J. Wikander, and B. Iliev, "Demonstration-based learning and control for automatic grasping," *Intell. Serv. Robot.*, vol. 2, Jan. 2009, doi: 10.1007/s11370-008-0026-3.
- [8] S. Ekvall and D. Kragic, "Interactive grasp learning based on human demonstration," in *IEEE International Conference on Robotics and Automation*, 2004. Proceedings. ICRA '04. 2004, Apr. 2004, vol. 4, pp. 3519–3524 Vol.4. doi: 10.1109/ROBOT.2004.1308798.
- [9] I. Lenz, H. Lee, and A. Saxena, "Deep Learning for Detecting Robotic Grasps," *Int. J. Robot. Res.*, vol. 34, Jan. 2013, doi: 10.1177/0278364914549607.
- [10] J. Bohg, A. Morales, T. Asfour, and D. Kragic, "Data-Driven Grasp Synthesis—A Survey," *IEEE Trans. Robot.*, vol. 30, no. 2, pp. 289–309, Apr. 2014, doi: 10.1109/TRO.2013.2289018.
- [11] P. Cerveri, E. De Momi, N. F. Lopomo, G. Baud-Bovy, R. Barros, and G. Ferrigno, "Finger Kinematic Modeling and Real-Time Hand Motion Estimation," *Ann. Biomed. Eng.*, vol. 35, pp. 1989–2002, Dec. 2007, doi: 10.1007/s10439-007-9364-0.
- [12] M. Gabbicini, G. Stillfried, H. Marino, and M. Bianchi, "A data-driven kinematic model of the human hand with soft-tissue artifact compensation mechanism for grasp synergy analysis," 2013. doi: 10.1109/IROS.2013.6696890.
- [13] J. R. Napier, "The prehensile movements of the human hand,," *J. Bone Joint Surg. Br.*, vol. 38-B 4, pp. 902–13, 1956.
- [14] M. R. Cutkosky, "On grasp choice, grasp models, and the design of hands for manufacturing tasks," *IEEE Trans. Robot. Autom.*, vol. 5, no. 3, pp. 269–279, Jun. 1989, doi: 10.1109/70.34763.
- [15] T. Feix, R. Pawlik, and H.-B. Schmiebmayer, "The generation of a comprehensive grasp taxonomy," Jan. 2009.
- [16] S. Ekvall and D. Kragic, "Learning and Evaluation of the Approach Vector for Automatic Grasp Generation and Planning," in *Proceedings 2007 IEEE International Conference on Robotics and Automation*, Apr. 2007, pp. 4715–4720. doi: 10.1109/ROBOT.2007.364205.
- [17] M. Santello, M. Flanders, and J. Soechting, "Postural Hand Synergies for Tool Use," *J. Neurosci. Off. J. Soc. Neurosci.*, vol. 18, pp. 10105–15, Dec. 1998, doi: 10.1523/JNEUROSCI.18-23-10105.1998.
- [18] F. Ficuciello, G. Palli, C. Melchiorri, and B. Siciliano, "A model-based strategy for mapping human grasps to robotic hands using synergies," 2013, p. 1742. doi: 10.1109/AIM.2013.6584348.
- [19] F. Ficuciello, A. Federico, V. Lippiello, and B. Siciliano, "Synergies Evaluation of the SCHUNK S5FH for Grasping Control," 2017.
- [20] M. Ciocarlie, C. Goldfeder, and P. Allen, "Dimensionality reduction for hand-independent dexterous robotic grasping," vol. 20. 2007, p. 3275. doi: 10.1109/IROS.2007.4399227.
- [21] F. Ficuciello, A. Migliozi, G. Laudante, P. Falco, and B. Siciliano, "Vision-based grasp learning of an anthropomorphic hand-arm system in a synergy-based control framework," *Sci. Robot.*, vol. 4, no. 26, 2019, doi: 10.1126/scirobotics.aao4900.
- [22] R. Balasubramanian, L. Xu, P. Brook, J. Smith, and Y. Matsuoka, "Physical Human Interactive Guidance: Identifying Grasping Principles From Human-Planned Grasps," *Robot. IEEE Trans. On*, vol. 28, pp. 899–910, Aug. 2012, doi: 10.1109/TRO.2012.2189498.
- [23] M. Ciocarlie and P. Allen, "Hand Posture Subspaces for Dexterous Robotic Grasping," *J Robot. Res.*, vol. 28, pp. 851–867, Jun. 2009, doi: 10.1177/0278364909105606.
- [24] Y. Li and N. S. Pollard, "A shape matching algorithm for synthesizing humanlike enveloping grasps," *5th IEEE-RAS Int. Conf. Humanoid Robots 2005*, pp. 442–449, 2005.
- [25] K. Huebner et al., "Grasping known objects with humanoid robots: A box-based approach," 2009, p. 6.
- [26] J. Bohg et al., "Mind the gap - Robotic grasping under incomplete observation," 2011, p. 693. doi: 10.1109/ICRA.2011.5980354.
- [27] F. Cini, V. Ortenzi, P. Corke, and M. Controzzi, "On the choice of grasp type and location when handing over an object," *Sci. Robot.*, vol. 4, no. 27, 2019, doi: 10.1126/scirobotics.aau9757. [28] Q. Lu and T. Hermans, "Modeling Grasp Type Improves Learning-Based Grasp Planning," *IEEE Robot. Autom. Lett.*, vol. PP, pp. 1–1, Jan. 2019, doi: 10.1109/LRA.2019.2893410.
- [28] Q. Lu and T. Hermans, "Modeling Grasp Type Improves Learning-Based Grasp Planning," *IEEE Robot. Autom. Lett.*, vol. PP, pp. 1–1, Jan. 2019, doi: 10.1109/LRA.2019.2893410.